Neurosci. Bull. August, 2019, 35(4):624–636
https://doi.org/10.1007/s12264-019-00345-0

www.neurosci.cn
www.springer.com/12264

ORIGINAL ARTICLE

Up-regulation of P2X7 Receptors Contributes to Spinal Microglial Activation and the Development of Pain Induced by BmK-I

Jingjing Zhou[1] · Xiaoxue Zhang[1] · You Zhou[1] · Bin Wu[1,2] · Zhi-Yong Tan[2]

Received: 2 August 2018 / Accepted: 13 October 2018 / Published online: 28 February 2019

Abstract Previous work has demonstrated that the sensitization of spinal neurons and microglia is important in the development of pain behaviors induced by BmK I, a Na^+ channel activator and a major peptide component of the venom of the scorpion *Buthus martensi* Karsch (BmK). We found that the expression of P2X7 receptors (P2X7Rs) was up-regulated in the ipsilateral spinal dorsal horn after BmK I injection in rats. P2X7R was selectively localized in microglia but not astrocytes or neurons. Similarly, interleukin 1β (IL-1β) was selectively up-regulated in microglia in the spinal dorsal horn after BmK I injection. Intrathecal injection of P2X7R antagonists largely reduced BmK I-induced spontaneous and evoked pain behaviors, and the up-regulation of P2X7R and IL-1β in the spinal cord. These data suggested that the up-regulation of P2X7Rs mediates microglial activation in the spinal dorsal horn, and therefore contributes to the development of BmK I-induced pain.

Keywords P2X7 receptor · BmK I · Spinal dorsal horn · Interleukin 1β · Microglia · Brilliant Blue G

✉ Zhi-Yong Tan
zt2@iupui.edu

[1] Laboratory of Neuropharmacology and Neurotoxicology, Shanghai University, Shanghai 200444, China

[2] Department of Pharmacology and Toxicology and Stark Neurosciences Research Institute, Indiana University School of Medicine, Indianapolis, IN 46202, USA

Introduction

Scorpion envenomation causes severe pain and is a serious public health problem in many countries [1]. In particular, envenomation by the scorpion *Buthus martensi* Karsch (BmK) can cause excruciating pain, skin edema, and a burning sensation at the site of the sting that can last for hours [2]. BmK I, a Na^+ channel activator and a major peptide component from the venom of the Asian scorpion BmK, has been shown to be a key mediator of inflammation and pain [3]. Intraplantar (i.pl.) injection of BmK I in rats induces spontaneous pain responses, ipsilateral thermal hypersensitivity, and bilateral (mirror-image) mechanical hypersensitivity [4]. The mirror-image mechanical hypersensitivity is a characteristic feature of the BmK I-induced pain model compared to other animal models of pain. Previous work from our lab has shown that BmK I induces hyperexcitability of dorsal root ganglion (DRG) neurons whose central termini are located in the spinal cord, and the sensitization of neurons in the spinal cord [5]. On the other hand, BmK I also activates microglial cells in the spinal cord [6]. However, it remains unknown how the increased neuronal activity leads to microglial activation and which receptor mediates microglial activation in the spinal dorsal horn and therefore contributes to the development of BmK I-induced pain.

P2X7 receptors (P2X7R) is a member of the ATP-sensitive ionotropic P2X receptor family which includes seven subtypes (P2X1-X7) [7]. P2X7Rs expressed in microglia play key roles in microglial activation and the subsequent release of pro-inflammatory cytokines, including interleukin-1β (IL-1β) and tumor necrosis factor-alpha (TNFα) in the spinal dorsal horn [8, 9]. Growing evidence has shown that P2X7R is important in the development of inflammatory and neuropathic pain [10]. For instance,

tetanic stimulation of the sciatic nerve induces the upregulation of P2X7Rs, which results in microglial activation, induction of spinal long-term potentiation, and persistent pain [11].

Taken together, the above results suggest that P2X7Rs might mediate the microglial activation caused by BmK I-induced neuronal hyperactivity and therefore contribute to the development of pain induced by BmK I. To evaluate the role of P2X7Rs in BmK I-induced pain, we investigated: (1) the effects of BmK I on the expression of P2X7Rs and IL-1β in the L4/5 spinal dorsal horn, (2) the localization of P2X7Rs and IL-1β in several types of spinal cells, (3) the effects of P2X7R antagonists on the development of BmK I-induced pain behaviors, and (4) the effects of P2X7R antagonists on the expression of spinal P2X7Rs and IL-1β.

Materials and Methods

Experimental Animals

Adult male Sprague-Dawley rats (200 g–220 g) were provided by the Shanghai Experimental Animal Center of the Chinese Academy of Sciences. All procedures complied with the guidelines provided by the International Association for the Study of Pain for pain research in conscious animals [12]. All animals had *ad libitum* access to food and water and were maintained in groups of two animals per cage. Animals were housed in a colony room maintained on a 12:12 h light-dark cycle at a constant temperature range of 23 °C–25 °C. All efforts were made to minimize animal suffering and reduce the number of animals used.

Preparation and Administration of BmK I

Crude BmK venom collected by electrical stimulation was purchased from a scorpion culture farm in Henan Province, China. As described by Ji *et al*., BmK I was purified from the crude venom using both high-performance liquid chromatography and mass spectrometry [3]. BmK I solution was prepared at a concentration of 0.2 μg/μL in physiological saline (0.9% NaCl). BmK I solution was then injected (50 μL i.pl.) into the left hind paw of each rat.

Drug Preparation and Administration

Brilliant Blue G (BBG; B0770-5G, Millipore Sigma Corp., St. Louis, MO) was dissolved in saline to 50 μmol/L, 100 μmol/L, or 300 μmol/L. Rats were anesthetized with sodium pentobarbital. Ten microliters of BBG or saline was administered intrathecally (i.t.) 30 min prior to BmK I administration. I.t. injection was achieved by direct lumbar puncture between L4 and L5 using a 25-μL Hamilton syringe connected to a 27-gauge, one-inch sterile disposable needle. Puncture of the dura was indicated by the formation of an S-shape by the tail.

Behavioral Testing

Spontaneous nociceptive responses, paw withdrawal mechanical threshold (PWMT), and paw withdrawal thermal latency (PWTL) were measured using the methods described by Bai *et al*. [4].

Measurement of Spontaneous Pain

Rats were individually placed in a transparent, Plexiglas test box (20 cm × 20 cm × 30 cm) and acclimatized for at least 30 min. Thirty minutes after i.t. injection of BBG or A-438079, BmK I was injected into the left hind paw. Hind paw flinches were taken as a measure of spontaneous pain behavior and were counted every 5 min for 2 h.

Measurement of PWMT

Rats were individually placed in a Plexiglas test box (20 cm × 20 cm × 30 cm) on a metal mesh floor (1-cm openings) and habituated to this environment for 30 min prior to testing. A series of 10 calibrated von Frey filaments (forces from 0.6 g to 26 g; 58011, Stoelting Co., Wood Dale, IL) was used to assess mechanical sensitivity. Individual filaments were applied to both hind paws from underneath the mesh floor. Each filament was probed for the same period (2 s–3 s) with an inter-stimulus interval of 10 s. A positive response was indicated by brisk withdrawal and/or flinching of the tested paw. Each rat's PWMT was defined as the lowest force that caused at least 5 withdrawals out of 10 consecutive applications [13]. The PWMT of control animals that did not show 5 withdrawals upon 10 test stimuli was defined as 26g. No higher force was applied to avoid potential injury. Baseline PWMT was measured in each rat 24 h prior to testing.

Measurement of PWTL

Each rat's PWTL to radiant heat stimuli was determined as previously described [13]. Heat stimuli were provided by a radiant heat stimulator (RTY-3, Xi'an Fenglan Instrument Factory, Xi'an) and consisted of a high-intensity, projector halogen lamp bulb (150 W, 24 V). Briefly, the lamp was placed directly under the glass floor of the testing cage 2 cm beneath the hind paw. Rats were placed in the testing box at least 30 min prior to the start of experimentation. The diameter of the light spot on the floor surface was

$\sim$ 3 mm. A maximum of 20 s of heat was set as the cut-off time to avoid tissue injury. Each rat received five stimuli at an inter-stimulus interval of 10 min. The PWTL was determined by averaging the values for the five consecutive stimuli. Baseline PWTL was measured in each rat 24 h prior to testing.

Western Blot

Rats were anesthetized with sodium pentobarbital (60 mg/kg, i.p.) and rapidly decapitated at the indicated time points after BmK I injection. Samples were homogenized in RIPA lysis buffer (Millipore Sigma Corp.) in an ice-water bath for 30 min. After centrifugation at 14,000 rpm for 15 min, the supernatant containing total cellular protein was collected. The protein concentration in each sample was determined using a Bradford assay kit according to the manufacturer's instructions (Biotechwell Co. Ltd., Shanghai). Proteins were separated on 5% SDS-PAGE and transferred to a PVDF membrane (0.45 μm; Millipore, Billerica, MA). The membranes were then incubated in 5% non-fat milk at room temperature for 2 h to prevent nonspecific binding. The following primary antibodies were then individually diluted in PBS with Tween-20 (PBST, 0.05% Tween-20) containing 1% BSA and incubated overnight at 4 °C: rabbit polyclonal antibody against P2X7R (1:1000, ab109054, Abcam, Cambridge, MA), rabbit polyclonal antibody against IL-1β (1:1500, ab9722, Abcam), and rabbit polyclonal antibody against actin (1:200, sc-1616, Santa Cruz Biotechnology, Inc., Dallas, TX). After washing in PBST, the membranes were probed with HRP-conjugated goat anti-rabbit IgG (H + L) antibody (1:10000, PAB002, Santa Cruz Biotechnology, Inc.) for 2 h at room temperature. Immunoblotting signals were detected using ECL reagents (WBKLS0050; Millipore) with a fully-automated chemiluminescence image analysis system (Tanon-5200; Tanon Science & Technology Co., Ltd., Shanghai). The bands were captured with the image analysis system and quantified using ImageJ (National Institutes of Health, Bethesda, MD).

Immunohistochemistry

At 2 h, 4 h, 8 h, and 24 h after injection of BmK I, rats were anesthetized and perfused intracardially with 200 mL of sterile saline, followed by 400 mL of fixative containing 4% paraformaldehyde in 0.1 mol/L phosphate buffer (PB, pH 7.4). Each rat's L4–L5 lumbar spinal cord tissue was post-fixed in the same fixative for 12 h at 4 °C. Then the tissues were dehydrated in 10% and 20% sucrose PB buffer in sequence until they sank, then placed in 30% sucrose PB buffer and dehydrated at 4 °C. Frozen serial coronal sections (15 μm thick) were cut on a cryostat microtome (HM525; Thermo Fisher Microm, Walldorf, Germany) and mounted on gelatin-coated glass slides.

Frozen sections were air-dried and incubated with 5% bovine serum albumin in PBS for 1 h at room temperature, followed by incubation with primary antibody diluents overnight at 4 °C. The primary antibodies used were as follows: rabbit polyclonal anti-P2X7R (1:400, ab109054, Abcam, Cambridge, MA), rabbit polyclonal anti-IL-1β (1:400, ab9722, Abcam), mouse monoclonal anti-NeuN (clone A60, 1:300, MAB377, Millipore Bioscience Research Reagents, Temecula, CA), mouse monoclonal anti-GFAP (1:300, GA5; Cell Signaling Technology, Danvers, MA), and goat polyclonal anti-Iba1 (1:300, ab107159, Abcam). The sections were then washed with 0.01 mol/L PBS before incubation with secondary antibodies. The secondary antibodies used were as follows: donkey anti-rabbit IgG H&L (AlexaFluor®555) (1:300, ab150074, Abcam), donkey anti-mouse IgG H&L (AlexaFluor®488) (1:300, ab150105, Abcam), donkey anti-goat IgG H&L (AlexaFluor®488) (1:300, ab150129, Abcam), donkey anti-mouse IgG H&L (AlexaFluor®594) (1:400, ab150108, Abcam), rhodamine (TRITC)-conjugated donkey anti-goat IgG(H + L) (1:500, SA00007-3, Proteintech Group, Inc., Rosemont, IL), and donkey anti-rabbit IgG-CFL 488 (1:200, sc-362261, Santa Cruz Biotechnology, Inc.). After 1.5 h incubation with the appropriate secondary antibodies, fluorescence microscopy was performed (Zeiss Lsm 710, Germany) and digital images were captured.

Real-Time Quantitative Polymerase Chain Reaction

Total RNA was isolated from the ipsilateral and contralateral L4–L5 spinal cord of adult male rats at 1 h, 2 h, 4 h, 8 h, and 24 h (n = 4 at each time point) after i.pl injection of 10 μL diluted BmK I solution (1 μg/μL) with Total RNA Extractor (TRIzol) (Sangon Biotech, Shanghai, China), then reverse-transcribed with Prime-Script® RT Master Mix (TaKaRa Bio Inc., Shiga, Japan), according to the manufacturer's protocol. Control rats were injected i.pl with 10 μL 0.9% saline and the RNA was isolated by the procedure described above. Primer sequences targeted to P2X7 were designed using Primer Premier 6.0 software (Premier Biosoft, Palo Alto, CA) and the primers for β-actin were designed referring to a previous publication [14]. All primers were synthesized by Sangon Biotech (Shanghai, China). The PCR primer sequences were as follows: P2X7-S: 5′-ACATCCTGGTTTTCGGCACT-3′; P2X7-A: 5′-AGGGCTCACAGCACTTACAG-3′; β-actin-S: 5′-AGCACTGTGTTGGCATAGAGGTC-3′; β-actin-A: 5′-ACTATCGGCAATGAGCGGTTCC-3′.

Quantitative PCR was performed in SYBR® remix Ex TaqTM (TaKaRa Bio Inc.) using the CFX Connect™

Real-Time PCR System (Bio-Rad, Hercules, CA). The mRNA of P2X7 subtypes was normalized to the β-actin mRNA level. Data were analyzed using the $2^{-\Delta\Delta Ct}$ method [15].

Statistical Analyses

All results are expressed as mean ± standard error of the mean (SEM) and were analyzed using GraphPad Prism 6 (GraphPad Software, Inc., La Jolla, CA). Data from immunostaining were analyzed with Image-Pro Plus 6.0 (Media Cybernetics, Inc. Rockville, MD). The differences between groups were compared by two-way ANOVA followed by Dunnett's *post hoc* test. The data from behavioral tests were analyzed using one-way ANOVA followed by Dunnett's *post hoc* test and two-way ANOVA followed by a Bonferroni's *post hoc* test. The relative densities of Western blots were analyzed by one-way ANOVA followed by Dunnett's *post hoc* test and one-way ANOVA followed by Tukey's *post hoc* test. $P < 0.05$ was considered to be statistically significant.

Results

BmK I Increased P2X7R Expression in Spinal Dorsal Horn

In control rats, a low P2X7R immunostaining intensity was detected in both the ipsilateral and contralateral dorsal horn (Fig. 1A, F). After injection of BmK I, the immunoreactive level of P2X7R was markedly increased in the ipsilateral dorsal horn (Fig. 1B–E, K). The increase in P2X7R was detected as early as 2 h, peaked at 4 h, decreased at 8 h, and returned toward baseline at 24 h after BmK I injection. In contrast, on the contralateral side, there was no significant increase in P2X7R at any of these time points (Fig. 1G–K). The pattern of increase in the P2X7R observed in the immunofluorescence experiments was paralleled by the results of Western blot experiments in the ipsilateral spinal cord (Fig. 1K, L). However, on the contralateral side, a significant increase in P2X7R was found from 1 h–24 h following BmK I injection in the Western blot compared to the immunofluorescence experiments (Fig. 1M). Moreover, the increase in P2X7R was higher at 8 h and 24 h, compared to 1 h–4 h after BmK I injection (Fig. 1M). To determine whether transcriptional mechanisms are involved in the upregulation of P2X7Rs, we conducted qPCR experiments. The results showed that P2X7R mRNA expression was selectively increased in the ipsilateral, but not the contralateral spinal cord (Fig. 1N, O). Significant increases were found at 2 h and 4 h after injection of BmK I.

Co-localization of P2X7Rs with Microglia in Spinal Dorsal Horn

To determine which types of spinal cells are involved in the upregulation of P2X7Rs after BmK I injection, we next performed double staining immunohistochemical experiments. Representative images of positive P2X7R staining are shown in Fig. 2A, E, and I. Double immunostaining for P2X7Rs with Iba-1 (a microglial marker), GFAP (an astrocytic marker), and NeuN (a neuronal marker) is shown in Fig. 2G–H, C–D, and K–L, respectively. Confocal microscopy and subsequent image analysis revealed that P2X7Rs were selectively co-localized with Iba-1-positive microglia (Fig. 2G, H), but not with either GFAP-positive astrocytes (Fig. 2C, D) or NeuN-positive neurons (Fig. 2K–L).

BmK I Increased IL-1β in the Spinal Dorsal Horn

To determine whether increased P2X7R levels result in increased expression of pro-inflammatory cytokines, we next measured the expression of IL-1β in the L4/5 dorsal horn. Immunostaining was performed before and after injection of BmK I. In control rats, the IL-1β immunostaining intensity was low (Fig. 3A, B). Four hours after BmK I injection, a large increase in IL-1β immunoreactivity was observed in both the ipsilateral and contralateral dorsal horn (Fig. 3C–F).

Additional Western blot analysis confirmed that IL-1β expression in both the ipsi- and contralateral dorsal horn was significantly increased after BmK I administration (Fig. 3G–H). On the ipsilateral and contralateral sides, a significant increase in IL-1β expression was detected at 4 h and 8 h following BmK I injection. However, the increase on the contralateral side persisted to 24 h after BmK I.

Co-localization of IL-1β with Microglia in Spinal Dorsal Horn

To determine which type of spinal cell is involved in the up-regulation of IL-1β after BmK I injection, we conducted double-staining immunohistochemical experiments. Representative images of positive IL-1β staining are shown in Fig. 4A, E, and I. Double immunostaining for IL-1β with Iba-1, GFAP, or NeuN is shown in Fig. 4G–H, C–D, and K–L, respectively. Confocal microscopy and subsequent image analysis revealed that IL-1β was selectively co-localized with Iba-1-positive microglia (Fig. 4G–H), but not with either GFAP-positive astrocytes (Fig. 4C–D) or NeuN-positive neurons (Fig. 4K–L).

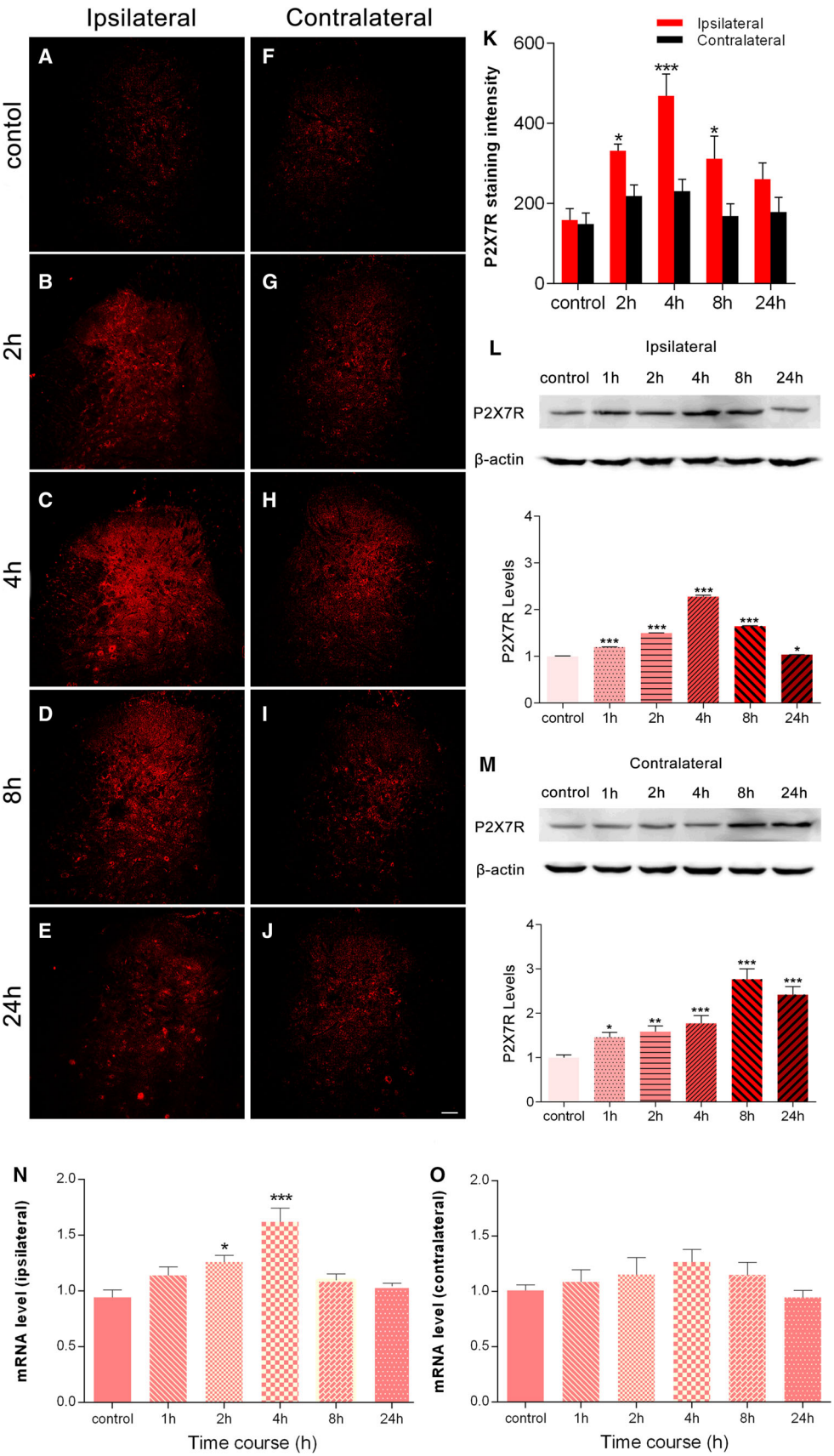

Fig. 1 BmK I injection induces P2X7R activation in spinal dorsal horn. **A**–**J** Spatiotemporal distribution of P2X7Rs in the dorsal horn in the presence of BmK I. Compared with the control group (**A**, **F**), the BmK I-treated groups (**B**–**E**, **G**–**J**) showed marked P2X7R immunoreactivity in the ipsilateral dorsal horn. Increased ipsilateral P2X7R immunoreactivity indicated that P2X7R activation began at 2 h, peaked at 4 h, and gradually decreased by 24 h after BmK I administration. Scale bar, 100 μm (**A**–**J**). **K** Statistic results of P2X7R expression in bilateral spinal cord ($n = 3$; $^{***}P < 0.001$, $^{*}P < 0.05$ compared with control, two-way ANOVA, Dunnett's *post hoc* test; error bars indicate SEM). **L**, **M** Western blots and analysis of P2X7Rs in spinal cord after intraplantar injection of BmK I. Representative Western blots show the expression of P2X7Rs and β-actin in the ipsilateral (**L**) and contralateral (**M**) spinal cord; histograms show mean levels with respect to each control group at different time points after intraplantar BmK I injection. **N**, **O** mRNA expression in the ipsilateral (**N**) and contralateral (**O**) spinal cord. The data are presented as mean ± SEM of four rats per group ($^{*}P < 0.05$, $^{**}P < 0.01$, $^{***}P < 0.001$ compared with control, one-way ANOVA, Dunnett's *post hoc* test).

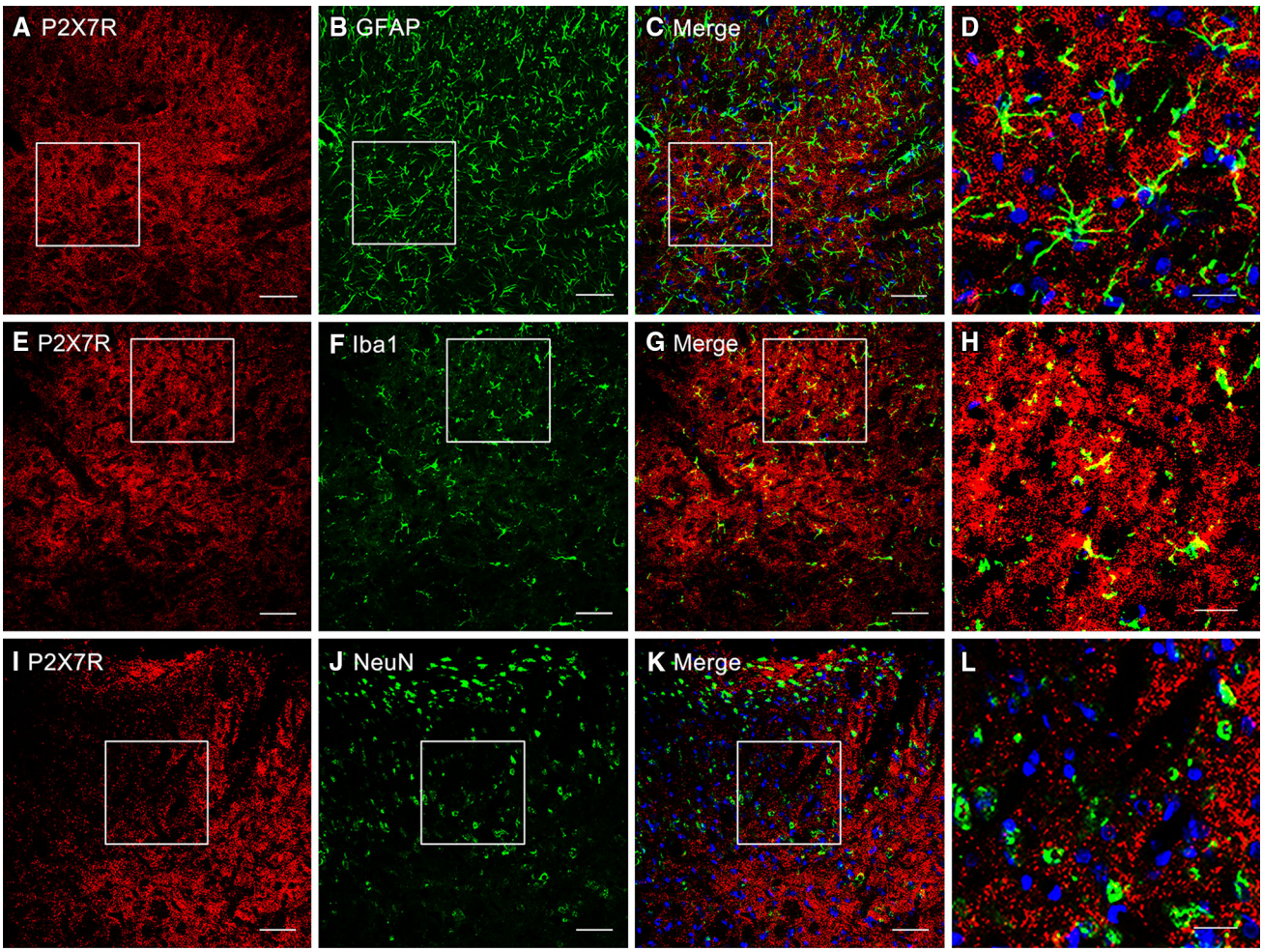

Fig. 2 Cellular localization of P2X7R immunoreactivity in the rat spinal dorsal horn. **A–L** Cell-type-specific immunolabeling of P2X7Rs in the ipsilateral dorsal horn at 4 h after intraplantar BmK I administration. (**A**, **E**, **I**) P2X7R-positive staining revealed no P2X7R co-localization with either the astrocytic marker GFAP or the neuronal marker NeuN (**B**, **C**, **J**, **K**). **F–G** Double immunofluorescence in the superficial dorsal horn showed that P2X7Rs co-localized with the microglial marker Iba-1. White open squares in **C**, **G**, **K** indicated the corresponding magnified images (**D**, **H**, **L**) in the confocal images. Scale bars, 50 μm in **A–C**, **E–G**, **I–K**; 20 μm in **D**, **H**, **L**.

P2X7R Antagonists Inhibited BmK I-Induced Pain Behaviors

BBG, a P2X7R antagonist, was used to test the involvement of P2X7Rs in BmK I-induced pain behaviors. Both spontaneous and evoked pain behaviors (mechanical and thermal) were studied. Either BBG or control (saline) was injected i.t. 30 min before BmK I administration. Compared with the control groups, all doses of BBG tested (50 μmol/L, 100 μmol/L, and 300 μmol/L) significantly reduced the spontaneous pain behavior at 5 min to 2 h after BmK I injection (Fig. 5A, B). The inhibition of spontaneous pain behaviors was dose-dependent from 50 μmol/L to 100 μmol/L BBG. No further inhibition occurred when the dosage was increased from 100 μmol/L to 300 μmol/L BBG. Similarly, BBG induced a dose-dependent inhibition of evoked pain behaviors (Fig. 5C–E). BBG largely inhibited BmK I-induced mechanical hypersensitivity in both the ipsilateral and contralateral hind paws at 4 h and 8 h after injection of BmK I (Fig. 5C, D). A similar inhibitory effect of BBG on ipsilateral thermal hypersensitivity was also found (Fig. 5E). On the other hand, neither BmK I nor BBG + BmK I significantly changed the baseline thermal threshold on the contralateral side (Fig. 5F).

To further test the role of P2X7R in BmK I-induced pain, we used a structurally different P2X7R antagonist, A-438079. Similarly, A-438079 inhibited both spontaneous and evoked pain behaviors induced by BmK I in a dose-dependent manner (Fig. 6). In contrast to BBG, 50 μmol/L A-438079 significantly inhibited ipsilateral mechanical and thermal hypersensitivity, and 300 μmol/L A-438079

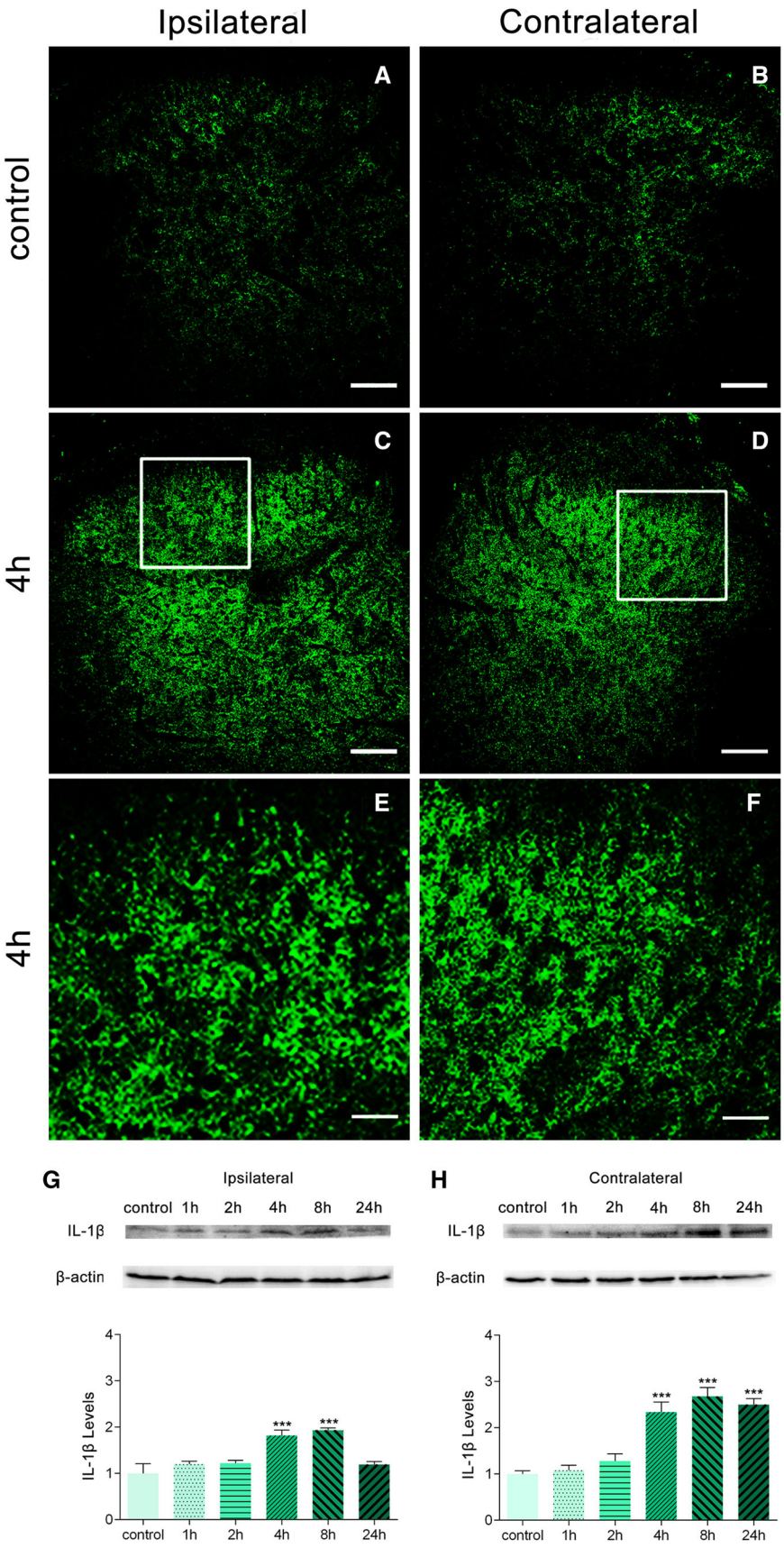

Fig. 3 Effects of BmK I on the release of IL-1β in the dorsal horn. Immunoreactivity of IL-1β in the rat spinal cord in the presence of BmK I. **A**–**F** Compared with the control group (**A**, **B**), bilateral IL-1β immunoreactivity in the dorsal horn increased significantly in BmK I-treated rats (**C**–**F**). White squares in **C** and **D** indicate the magnified images in **E** and **F**. Scale bars, 100 μm in **A**–**D**; 50 μm in **E**, **F**. **G**–**H** Representative Western blots of IL-1β and β-actin in the ipsilateral (**G**) and contralateral (**H**) spinal cord; histograms show the mean levels with respect to each control group at different time points after intraplantar BmK I injection. The data are presented as mean ± SEM ($n = 3$; $^{***}P < 0.001$ compared with control, one-way ANOVA followed by Dunnett's *post hoc* test).

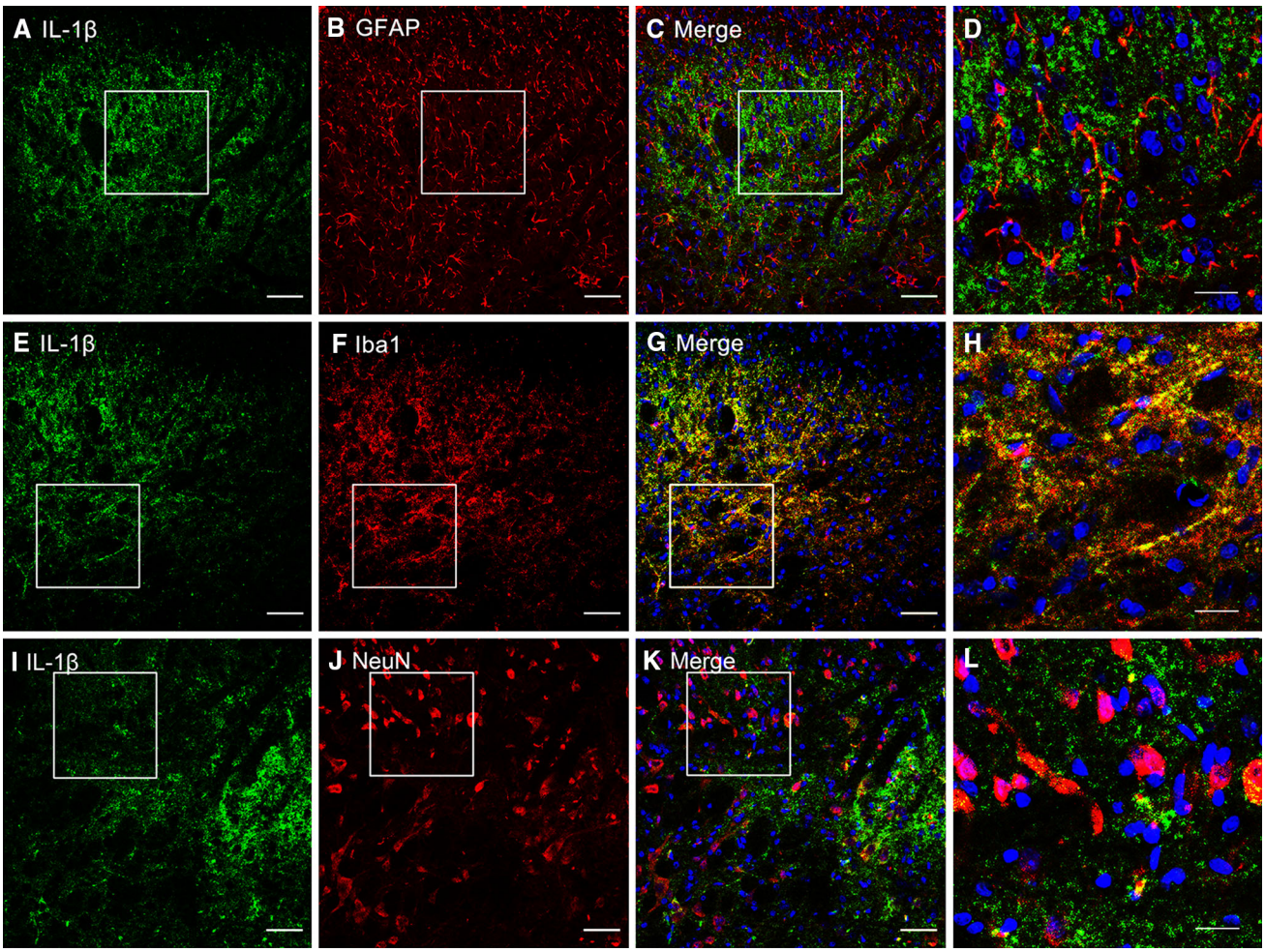

Fig. 4 Cellular localization of IL-1β immunoreactivity in the dorsal horn. **A–L** Cell-type-specific immunolabeling of IL-1β in the ipsilateral dorsal horn at 4 h after intraplantar BmK I. **A**, **E**, **I** IL-1β-positive staining. **B**, **C**, **J**, **K** Absence of IL-1β co-localization with either the astrocytic marker GFAP or the neuronal marker NeuN. **F–G** Double immunofluorescence in the superficial dorsal horn showing co-localization of IL-1β with the microglial marker Iba-1. White open squares in **C**, **G**, **K** indicate the magnified images in **D**, **H**, **L**. Scale bars, 50 μm in **A–C**, **E–G**, **I–K**; 20 μm in **D**, **H**, **L**.

induced a level of inhibition of evoked pain behaviors similar to that of 100 μmol/L A-438079 (Fig. 6).

BBG Inhibited BmK I-Induced Up-Regulation of P2X7R and IL-1β in Spinal Dorsal Horn

Both immunofluorescence and Western blot experiments were performed at 4 h after BmK I administration. In both experiments, BmK I significantly increased the expression of P2X7Rs (Fig. 7A–D) and IL-1β (Fig. 7E–H) in the dorsal horn. Pre-treatment with BBG significantly inhibited the expression of both P2X7Rs (Fig. 7A–D) and IL-1β (Fig. 7E–H) in the dorsal horn.

Discussion

Up-regulation of Microglial P2X7Rs and IL-1β in the Spinal Cord in BmK I-Induced Pain

In the present study, we found that P2X7R was selectively increased in the ipsilateral dorsal horn using immunofluorescence. We also found that P2X7Rs were increased in both the ipsilateral and contralateral spinal cord using Western blots. The difference in results between these experiments might be due to the fact that the immunofluorescence experiments focused only on the dorsal spinal cord while the Western experiments included both the dorsal and ventral spinal cord. Because P2X7Rs are also expressed in the ventral horn of the rat lumbar spinal cord, our results suggested that, in addition to an ipsilateral increase of P2X7Rs in the dorsal horn, BmK I might also

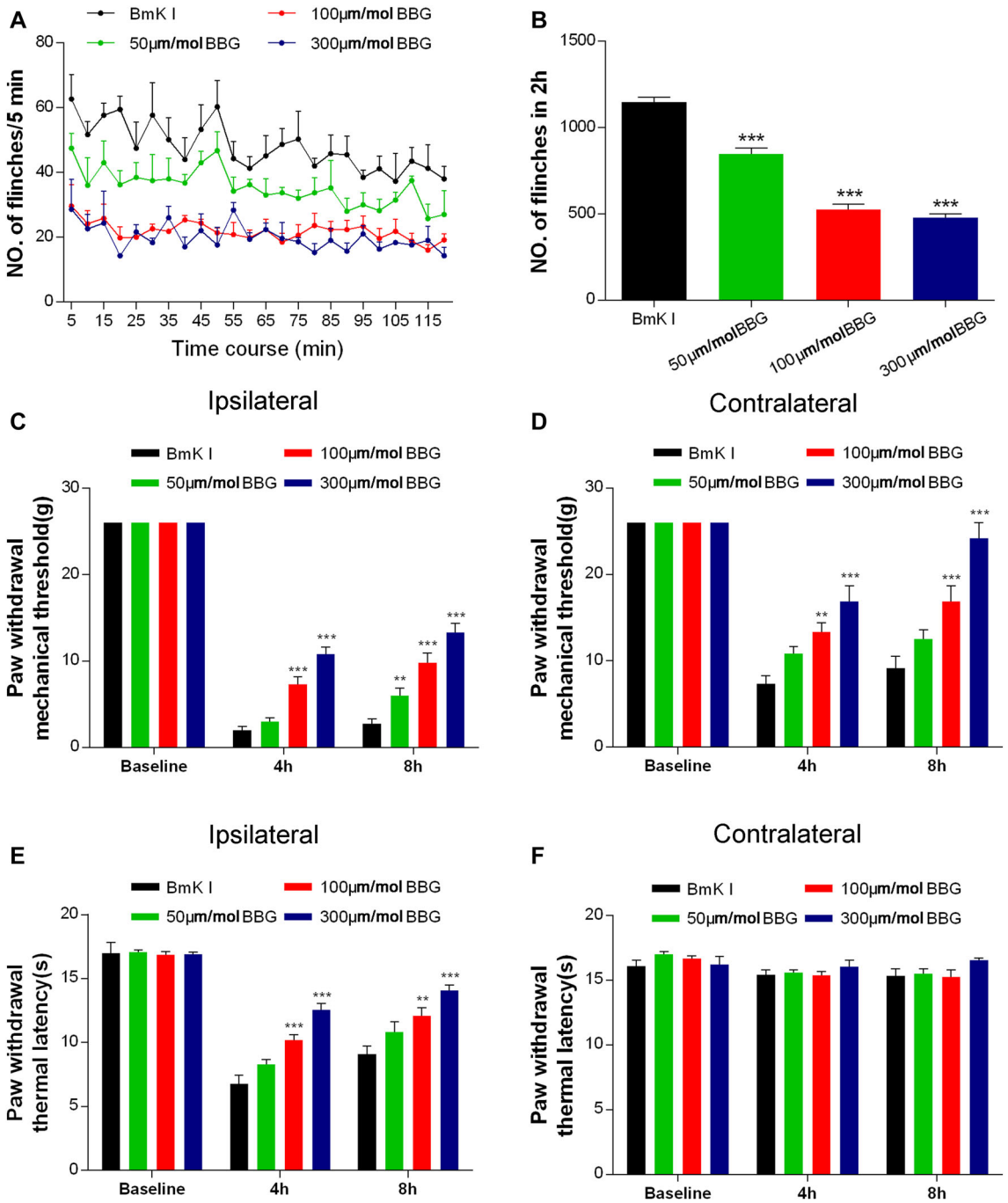

Fig. 5 P2X7R antagonist BBG reduced BmK I-induced pain. **A** Pain behavior was attenuated after BBG pretreatment at 50 μmol/L, 100 μmol/L, and 300 μmol/L, 30 min before BmK I administration. **B** Reduction in the total number of paw flinches after BBG pretreatment at the above doses in 2 h after BmK I injection. **C**–**F** Dose-dependent BBG-induced reduction of the ipsilateral (**C**) and contralateral (**D**) mechanical hypersensitivity as well as the ipsilateral thermal hypersensitivity (**E**). BBG did not affect the contralateral basal thermal latency (**F**). $n = 6$/group; $^{**}P < 0.01$, $^{***}P < 0.001$ compared with saline control group, one-way ANOVA, Dunnett's *post hoc* test and two-way ANOVA, Bonferroni's *post hoc* test.

induce a contralateral increase of P2X7Rs in the ventral horn. On the other hand, increased P2X7R mRNA expression might contribute to the increased protein expression on the ipsilateral, but not the contralateral side. Nevertheless, the nature and the potential consequences of this contralateral increase of P2X7Rs in the ventral horn are beyond the scope of the present study and need further studies to explore.

It has been reported that the expression of P2X7Rs in spinal microglia is up-regulated in several models of

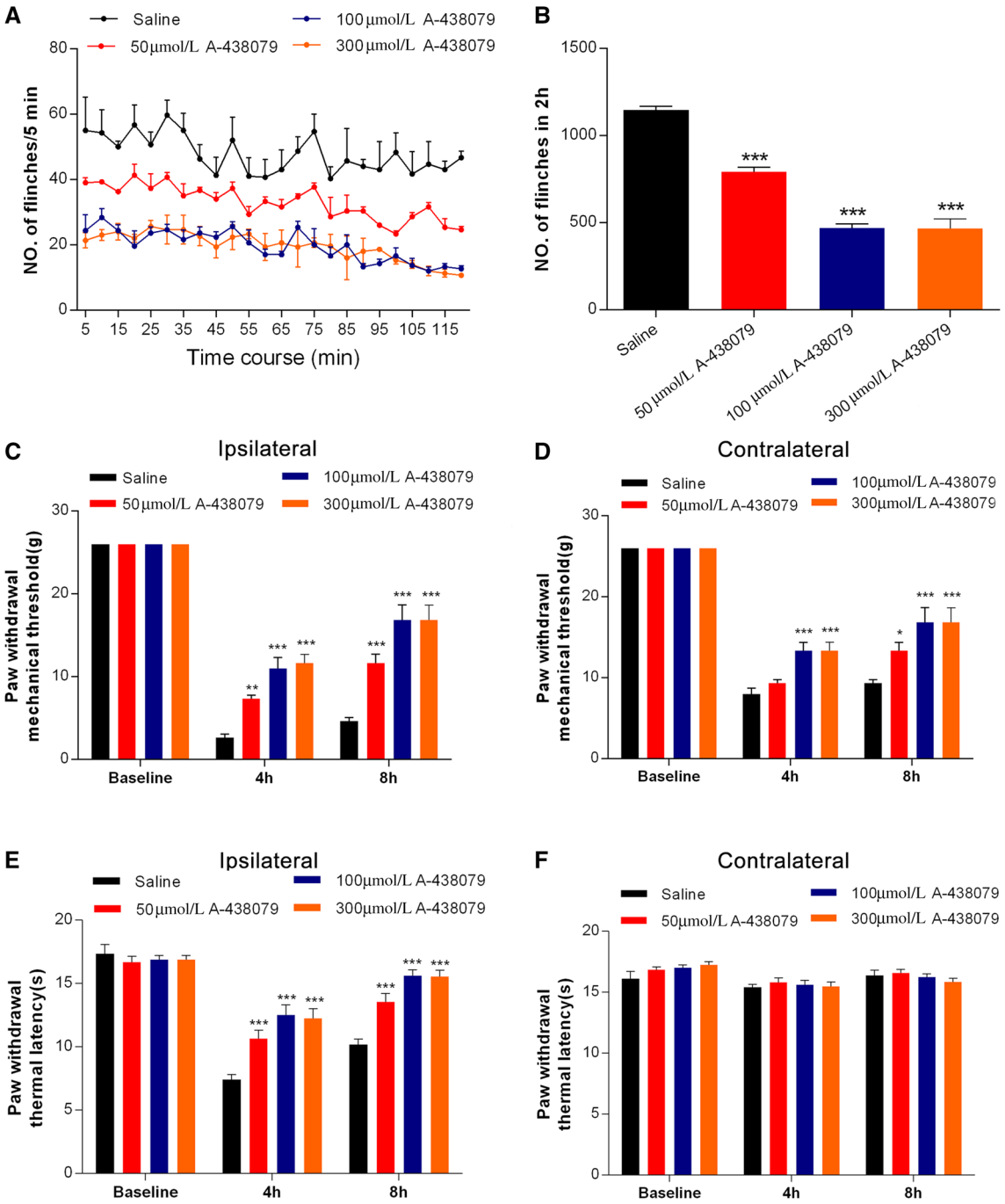

Fig. 6 P2X7R antagonist A-438079 reduced BmK I-induced pain. **A** Pain behavior was attenuated after A-438079 pretreatment at 50 μmol/L, 100 μmol/L, and 300 μmol/L, 30 min before BmK I administration. **B** Reduction in the total number of paw flinches after A-438079 pretreatment at the above doses in the 2 h after BmK I injection. **C**–**F** A-438079 reduced the ipsilateral (**C**) and contralateral (**D**) mechanical hypersensitivity as well as the ipsilateral thermal hypersensitivity (**E**). A-438079 did not affect the contralateral basal thermal latency (**F**). $n = 6$/group; $^{*}P < 0.05$, $^{**}P < 0.01$, $^{***}P < 0.001$ compared with saline control group, one-way ANOVA, Dunnett's *post hoc* test and two-way ANOVA, Bonferroni's *post hoc* test.

neuropathic and inflammatory pain [16–18]. Similar to these models, we found a preferential increase of P2X7Rs in the microglia in the ipsilateral spinal cord in the BmK I model. However, the increase of P2X7Rs in the BmK I model was much faster than that in other models. In the BmK I model, P2X7Rs increased within hours after injection of BmK I. In contrast, increases in P2X7Rs occur within days after surgery in models using chronic constriction of the sciatic nerve injury (SNI) [16] and postsurgical pain [18]. Interestingly, both the mRNA and

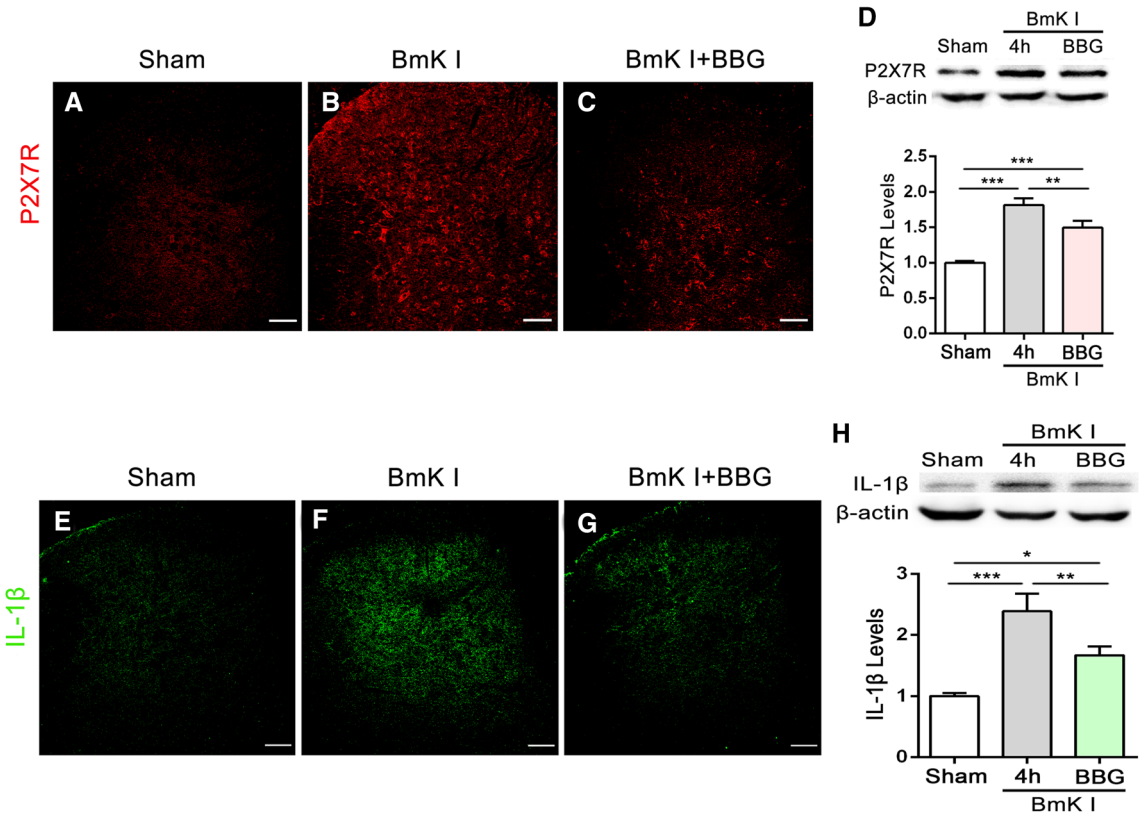

Fig. 7 Effects of BBG on the activation of P2X7Rs and the release of IL-1β in the spinal dorsal horn in the presence of BmK I. Representative P2X7R and IL-1β immunofluorescence labeling at 4 h following sham (**A**, **E**) and BmK I stimulation in the saline and BBG injection groups (**B**–**C**, **F**–**G**). Scale bars, 100 μm. Western blot analysis showed that the BmK I-induced up-regulation of P2X7Rs (**D**) and IL-1β (**H**) was inhibited by BBG treatment (100 μmol/L, 30 min before BmK I injection; n = 3/group; $^{*}P < 0.05$, $^{**}P < 0.01$, $^{***}P < 0.001$ compared with sham, one-way ANOVA, Tukey's *post hoc* test).

protein expression of P2X7Rs were increased within hours after BmK I injection. These results suggested that increased mRNA contributes to the rapid increase in protein. However, these results did not exclude other mechanisms, such as cell trafficking, which might also be involved in the rapid increase of P2X7Rs following BmK I injection.

It has been reported that the activation of P2X7Rs by ATP elicits the release of inflammatory cytokines such as IL-1β and TNF-α from microglia [19–22]. Here, we found that the expression of IL-1β was significantly increased in both the ipsilateral and contralateral dorsal horn following BmK I injection. However, P2X7Rs only increased on the ipsilateral side. Therefore, our results suggested that the up-regulation of P2X7Rs contributes to the production of IL-1β on the ipsilateral spinal cord. It remains unknown whether the ipsilateral increase of P2X7Rs contributes to the contralateral increase in IL-1β or how the contralateral increase of IL-1β is caused. Moreover, on the ipsilateral side, the increase of both P2X7R and IL-1β returned to the normal level within 24 h after BmK I injection. However, BmK I-induced ipsilateral pain behaviors persist for > 24 h [4]. These results suggested that the activation of P2X7Rs and the release of IL-1β selectively contribute to the early phase of BmK I-induced pain. On the other hand, increased P2X7Rs and IL-1β might also trigger the activation of other signal cascades in the spinal cord and thereby contribute to the development of BmK I-induced pain that lasts beyond 24 h after BmK I injection.

Previous studies from our lab have demonstrated that BmK I sensitizes DRG neurons whose central projections are located in the spinal cord, and both neurons and glia in the spinal cord [6, 23, 24]. BmK I up-regulates the expression of sodium channel 1.8 (Nav1.8), Akt, and mTOR in DRG neurons [23, 25, 26]. In the spinal cord, BmK I induces the expression of c-Fos, increases the release of excitatory amino-acids, and up-regulates 5-HT_{3A} receptors in neurons [24, 27]. BmK I also activates microglia and microglial p38 in the spinal cord [6]. The present study provides a possible mechanism underlying the cross-talk between neurons and glia in the dorsal horn in the BmK I-induced pain model. Our results suggest that increased P2X7Rs mediate neuronal sensitization-induced microglial activation in the dorsal horn. Also, the increased

IL-1β might contribute to the neuronal sensitization induced by microglial activation. Therefore, increases of P2X7Rs and IL-1β in microglia might function at the input and output side, respectively, of microglial interaction with neurons in the spinal cord.

It has been reported that the P2X7R contributes to p38 activation, and/or the subsequent production of IL-1β in microglia in a couple of pain models [11, 28]. Our previous study showed that microglial p38 is activated after BmK I injection [6]. Combined with the results in the present study, these findings suggest that the up-regulation of P2X7Rs contributes to p38 activation and subsequent over-expression of IL-1β in microglia after BmK I injection.

P2X7R Antagonists Inhibited BmK I-Induced Pain Behaviors and the Up-regulation of P2X7Rs and IL-1β

Microglial P2X7R plays an important role in the development of pathological pain. Knockout of P2X7R dramatically reduces the production of pro-inflammatory cytokines including IL-1β, and completely blocks the development of both inflammatory and neuropathic pain [10]. Antagonists of P2X7R suppress the development of mechanical hypersensitivity in animal pain models of SNI, CCI, and postsurgical pain. In the latter two models, it was also found that the P2X7R antagonists inhibit the activation of microglia [16, 18]. In the present study, we found that P2X7R antagonists (BBG and A-438079) largely inhibited the spontaneous and evoked pain behaviors induced by BmK I. Moreover, pre-treatment with BBG also reduced the expression of P2X7Rs and IL-1β. Interestingly, the inhibitory effects of BBG on P2X7R expression have also been found in tetanic stimulation [11]. These results suggest that P2X7R antagonists inhibit BmK I-induced pain through suppression of both function and expression of P2X7R, and the subsequent microglial activation and the release of neuro-excitatory molecules. On the other hand, these results also suggest that a positive feedback mechanism might underlie the P2X7R activation-induced up-regulation of P2X7Rs. Although no study has demonstrated such a mechanism, it might be speculated that the activation of p38 and/or production of cytokines such as IL-1β could contribute to the positive feedback effect.

It has been reported that BBG also inhibits Na^+ channels. However, the IC_{50} for BBG to block P2X7Rs is in the range of 10 nmol/L to 200 nmol/L [29], while the IC_{50} for BBG to block Na^+ currents is in the micromolar range [30]. Therefore, the effects of BBG on the pain behaviors and expression of P2X7Rs and IL-1β were most likely to be mediated *via* P2X7Rs in the current study. This suggestion was also supported by the similar effects of another P2X7R antagonist, A-438079. On the other hand, a possible contribution of Na^+ channels cannot be completely ruled out in the BBG experiment.

Conclusions

In summary, we found that peripheral administration of BmK I induced the up-regulation of P2X7Rs and the pro-inflammatory cytokine IL-1β, predominantly in spinal microglia. Pretreatment with P2X7R antagonists prevented the BmK I-induced spontaneous and evoked pain behaviors, and the up-regulation of P2X7Rs and IL-1β in spinal microglia. These results suggest that P2X7Rs mediate BmK I-induced microglial activation, and therefore contribute to the development of BmK I-induced inflammatory pain through pro-inflammatory cytokines.

Acknowledgements This work was supported by grants from the National Natural Science Foundation of China (31571032 and 31771191). Zhi-Yong Tan was supported by an Indiana Spinal Cord and Brain Injury Research Fund grant from Indiana State Department of Health, USA (2017).

References

1. Amitai Y. Clinical manifestations and management of scorpion envenomation. Public Health Rev 1998, 26: 257–263.
2. Goudet C, Chi CW, Tytgat J. An overview of toxins and genes from the venom of the Asian scorpion Buthus martensi Karsch. Toxicon 2002, 40: 1239–1258.
3. Ji YH, Mansuelle P, Terakawa S, Kopeyan C, Yanaihara N, Hsu K, *et al.* Two neurotoxins (BmK I and BmK II) from the venom of the scorpion Buthus martensi Karsch: purification, amino acid sequences and assessment of specific activity. Toxicon 1996, 34: 987–1001.
4. Bai ZT, Liu T, Jiang F, Cheng M, Pang XY, Hua LM, *et al.* Phenotypes and peripheral mechanisms underlying inflammatory pain-related behaviors induced by BmK I, a modulator of sodium channels. Exp Neurol 2010, 226: 159–172.
5. Ye P, Jiao Y, Li Z, Hua L, Fu J, Jiang F, *et al*. Scorpion toxin BmK I directly activates Nav1.8 in primary sensory neurons to induce neuronal hyperexcitability in rats. Protein Cell 2015, 6: 443–452.
6. Niu QS, Jiang F, Hua LM, Fu J, Jiao YL, Ji YH, *et al.* Microglial activation of p38 contributes to scorpion envenomation-induced hyperalgesia. Biochem Biophys Res Commun 2013, 440: 374–380.
7. North RA. Molecular physiology of P2X receptors. Physiol Rev 2002, 82: 1013–1067.
8. Skaper SD. Ion channels on microglia: therapeutic targets for neuroprotection. CNS Neurol Disord Drug Targets 2011, 10: 44–56.
9. Volonte C, Apolloni S, Skaper SD, Burnstock G. P2X7 receptors: channels, pores and more. CNS Neurol Disord Drug Targets 2012, 11: 705–721.
10. Chessell IP, Hatcher JP, Bountra C, Michel AD, Hughes JP, Green P, *et al.* Disruption of the P2X7 purinoceptor gene abolishes chronic inflammatory and neuropathic pain. Pain 2005, 114: 386–396.

11. Chu YX, Zhang Y, Zhang YQ, Zhao ZQ. Involvement of microglial P2X7 receptors and downstream signaling pathways in long-term potentiation of spinal nociceptive responses. Brain Behav Immun 2010, 24: 1176–1189.
12. Zimmermann M. Ethical guidelines for investigations of experimental pain in conscious animals. Pain 1983, 16: 109–110.
13. Jiang F, Pang XY, Niu QS, Hua LM, Cheng M, Ji YH. Activation of mammalian target of rapamycin mediates rat pain-related responses induced by BmK I, a sodium channel-specific modulator. Mol Pain 2013, 9: 50.
14. Qin S, Jiang F, Zhou Y, Zhou G, Ye P, Ji Y. Local knockdown of Nav1.6 relieves pain behaviors induced by BmK I. Acta Biochim Biophys Sin (Shanghai) 2017, 49: 713–721.
15. Adnan M, Morton G, Hadi S. Analysis of rpoS and bolA gene expression under various stress-induced environments in planktonic and biofilm phase using 2(-Delta Delta CT) method. Mol Cell Biochem 2011, 357: 275–282.
16. He WJ, Cui J, Du L, Zhao YD, Burnstock G, Zhou HD*, et al.* Spinal P2X(7) receptor mediates microglia activation-induced neuropathic pain in the sciatic nerve injury rat model. Behav Brain Res 2012, 226: 163–170.
17. Kobayashi K, Takahashi E, Miyagawa Y, Yamanaka H, Noguchi K. Induction of the P2X7 receptor in spinal microglia in a neuropathic pain model. Neurosci Lett 2011, 504: 57–61.
18. Ying YL, Wei XH, Xu XB, She SZ, Zhou LJ, Lv J*, et al.* Overexpression of P2X7 receptors in spinal glial cells contributes to the development of chronic postsurgical pain induced by skin/muscle incision and retraction (SMIR) in rats. Exp Neurol 2014, 261: 836–843.
19. Bianco F, Pravettoni E, Colombo A, Schenk U, Moller T, Matteoli M*, et al.* Astrocyte-derived ATP induces vesicle shedding and IL-1 beta release from microglia. J Immunol 2005, 174: 7268–7277.
20. Brough D, Le Feuvre RA, Iwakura Y, Rothwell NJ. Purinergic (P2X7) receptor activation of microglia induces cell death via an interleukin-1-independent mechanism. Mol Cell Neurosci 2002, 19: 272–280.
21. Chakfe Y, Seguin R, Antel JP, Morissette C, Malo D, Henderson D*, et al.* ADP and AMP induce interleukin-1beta release from microglial cells through activation of ATP-primed P2X7 receptor channels. J Neurosci 2002, 22: 3061–3069.
22. Song J, Ying Y, Wang W, Liu X, Xu X, Wei X, *et al*. The role of P2X7R/ERK signaling in dorsal root ganglia satellite glial cells in the development of chronic postsurgical pain induced by skin/muscle incision and retraction (SMIR). Brain Behav Immun. 2018, 69: 180–189.
23. Jiang F, Hua LM, Jiao YL, Ye P, Fu J, Cheng ZJ*, et al.* Activation of mammalian target of rapamycin contributes to pain nociception induced in rats by BmK I, a sodium channel-specific modulator. Neurosci Bull 2014, 30: 21–32.
24. Bai ZT, Zhang XY, Ji YH. Fos expression in rat spinal cord induced by peripheral injection of BmK I, an alpha-like scorpion neurotoxin. Toxicol Appl Pharmacol 2003, 192: 78–85.
25. Ye P, Hua L, Jiao Y, Li Z, Qin S, Fu J*, et al.* Functional upregulation of Nav1.8 sodium channel on dorsal root ganglia neurons contributes to the induction of scorpion sting pain. Acta Biochim Biophys Sin (Shanghai) 2016, 48: 132–144.
26. Zhou G, Jiao Y, Zhou Y, Qin S, Tao J, Jiang F*, et al.* Upregulation of Akt and Nav1.8 in BmK I-induced pain. Neurosci Bull 2018, 34: 539–542.
27. Fu J, Jiao YL, Li ZW, Ji YH. Spinal 5-HT3AR contributes to BmK I-induced inflammatory pain in rats. Sheng Li Xue Bao 2015, 67: 283–294.
28. Yang Y, Li H, Li TT, Luo H, Gu XY, Lu N*, et al.* Delayed activation of spinal microglia contributes to the maintenance of bone cancer pain in female Wistar rats via P2X7 receptor and IL-18. J Neurosci 2015, 35: 7950–7963.
29. Jiang LH, Mackenzie AB, North RA, Surprenant A. Brilliant blue G selectively blocks ATP-gated rat P2X(7) receptors. Mol Pharmacol 2000, 58: 82–88.
30. Jo S, Bean BP. Inhibition of neuronal voltage-gated sodium channels by brilliant blue G. Mol Pharmacol 2011, 80: 247–257.